

Supporting Information

Ordered Mesoporous Crystalline γ -Al₂O₃ with Variable Architecture and Porosity from a Single Hard-Template

Zhangxiong Wu †, ‡, *Qiang Li* ‡, *Dan Feng* ‡, *Paul A. Webley* †, and *Dongyuan*

*Zhao** †, ‡

† Department of Chemical Engineering, Monash University, Clayton, VIC 3800, Australia; ‡ Department of Chemistry and Laboratory of Advanced Materials, Fudan University, Shanghai 200433, P. R. China.

Email: dongyuan.zhao@eng.monash.edu.au and dyzhao@fudan.edu.cn, Tel: 61-3-9905-4174, Fax: 61-3-9905-5686

Experimental details for the evaluation of surface acidity and basicity

The acidity and basicity of the typical ordered mesoporous alumina material, OMA-2-FMC, were evaluated through adsorption/desorption of ammonia and carbon dioxide, respectively, which was similar to temperature programmed desorption (TPD) experiments. Typically, ~ 10 mg of the alumina sample was put in a small crucible and placed in the chamber of a TG unit. The sample was first activated at 500 °C (5 °C/min) for 2 h under N₂ (99.999 %, 20 ml/min). Then the chamber was cooled down to 180 °C for ammonia adsorption or 120 °C for carbon dioxide adsorption. At this stage, the N₂ gas was replaced by a ~ 5 % (v/v) NH₃ in helium gas mixture (20 ml/min) or a pure CO₂ gas (15 ml/min), and the temperature was kept isothermal at 180 or 120 °C for 60 min to achieve adsorption equilibrium. Then, the active gas was

switched back to N₂ while keep the temperature steady. The system was purged for 30 min under N₂ to remove the weakly adsorbed NH₃ or CO₂. After purging, the temperature was elevated to 600 °C to measure the TPD property of NH₃ or CO₂, both with a ramp rate of 5 °C/min. Blank experiments both for NH₃ and CO₂ adsorption were also run for calibration. The weight changes of the samples during the whole procedure were continuously recorded, from which the NH₃ or CO₂ adsorbed amounts were retrieved.

FIIR spectra of pyridine adsorption measurements: approximately 10 mg of OMA-2-FMC powder sample was pressed into a self-supported disc (2 cm in diameter). The sample was first activated at 300 °C for 2 h under vacuum. After cooling to 25 °C, pyridine vapor was introduced into the system with a pressure of ~ 133 Pa for adsorption with a duration of 1 h to achieve equilibrium. Then, the system was evacuated at different temperatures (25 ~ 300 °C) with intervals of 50 °C from 100 to 300 °C for 0.5 h. Transmission IR spectra at different conditions were recorded in the 400 ~ 4000 cm⁻¹ range with a 4 cm⁻¹ resolution on a Nicolet Nexus 470 spectrometer.

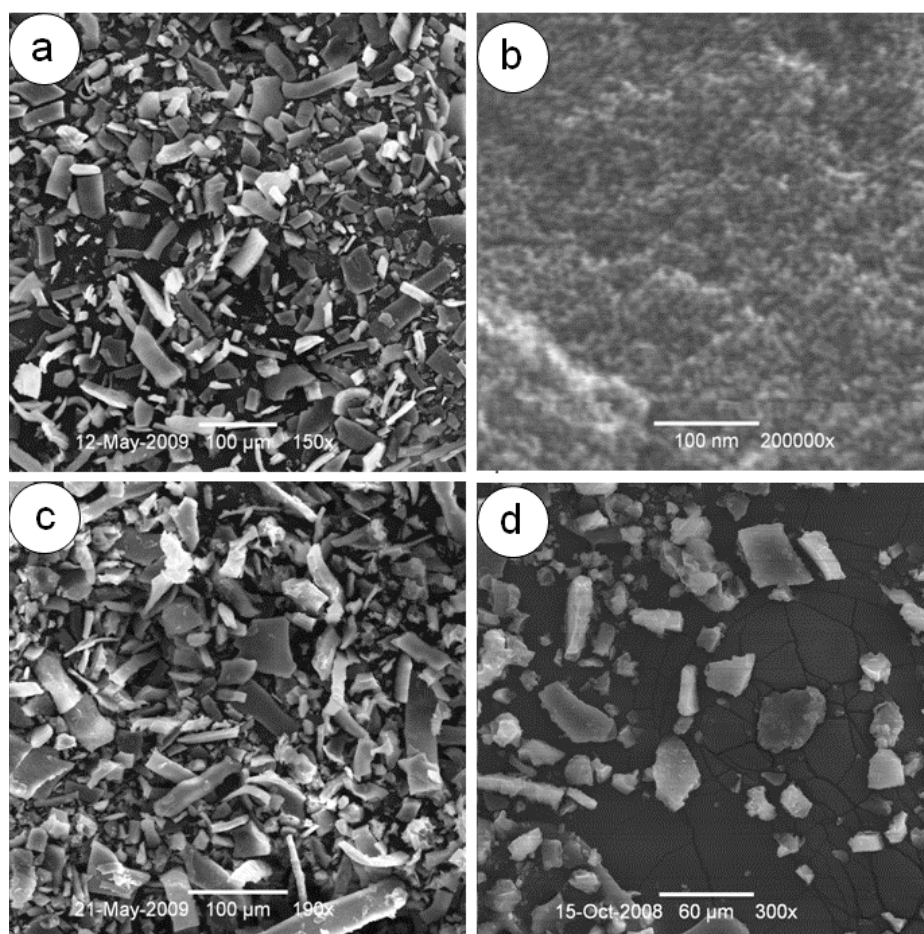


Figure S1. SEM images of the functionalized mesoporous carbon (FMC) template (a, b), the mesoporous alumina OMA-2-FMC (c) and OMA-3-FMC materials (d), respectively. It is obvious that all of the three materials show the similar flake-like morphology and pore arrangement. However, the two mesoporous alumina materials have lower structural regularity compared to the carbon hard-template.

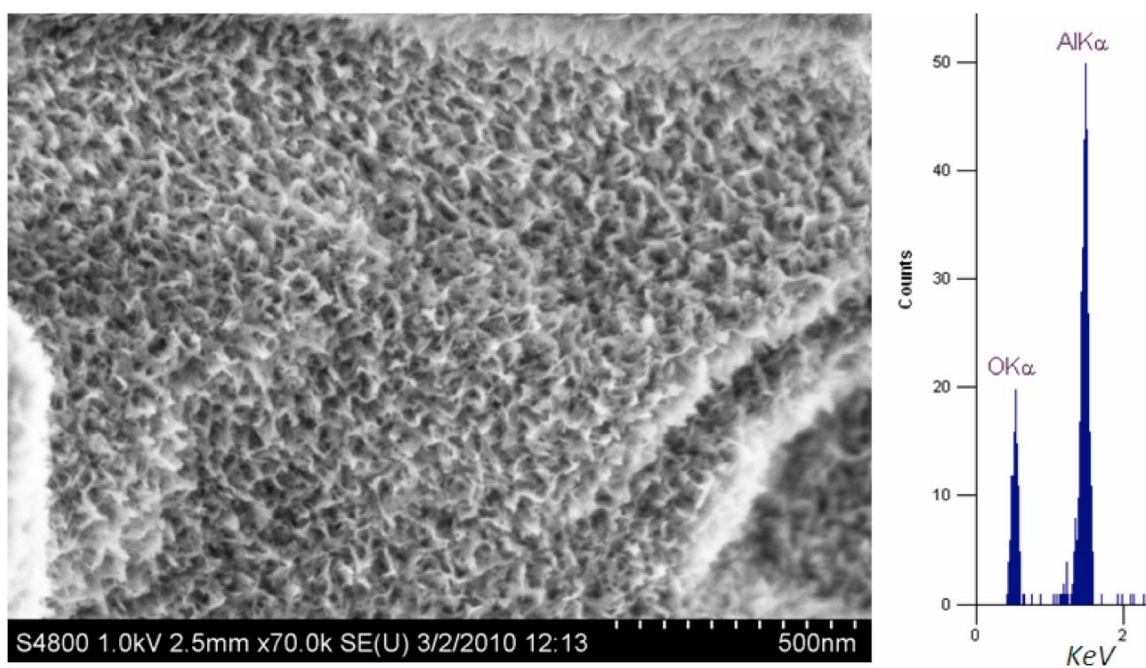


Figure S2. The HR-SEM image (left) of the corresponding side view of the ordered [100] domain of the mesoporous alumina OMA-2-FMC presented in Figure 1a, and the corresponding EDX pattern (right). It is clearly shown that the pore network is composed of tubular mesopores. From the EDX pattern, the OMA-2-FMC material is only composed of Al and O with a molar ratio very close to 2: 3.

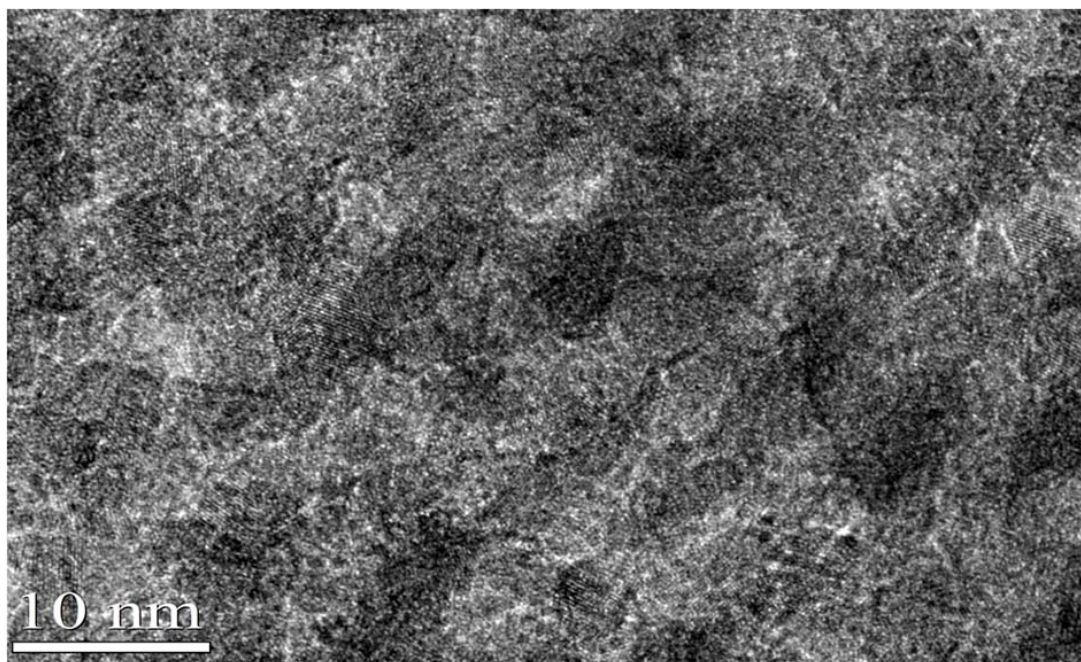


Figure S3. The HR-TEM image of the ordered mesoporous alumina OMA-2-FMC, clearly showing the coexistence of ordered mesostructure and γ -alumina nanocrystals.

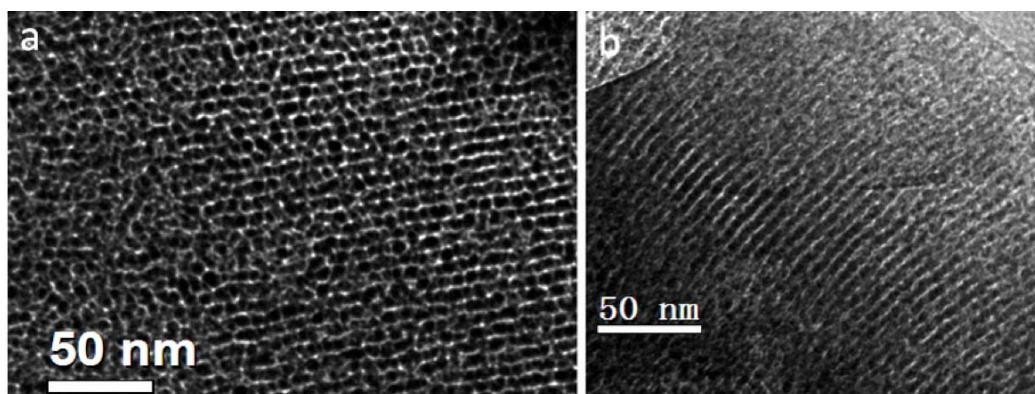


Figure S4. Comparison of TEM images of the mesoporous alumina materials, (a), OMA-2-FMC; (b), OMA-3-FMC. It obviously shows much more complementary pores penetrating the cylindrical mesopore walls in the sample OMA-2-FMC (a) than those in the sample OMA-3-FMC (b).

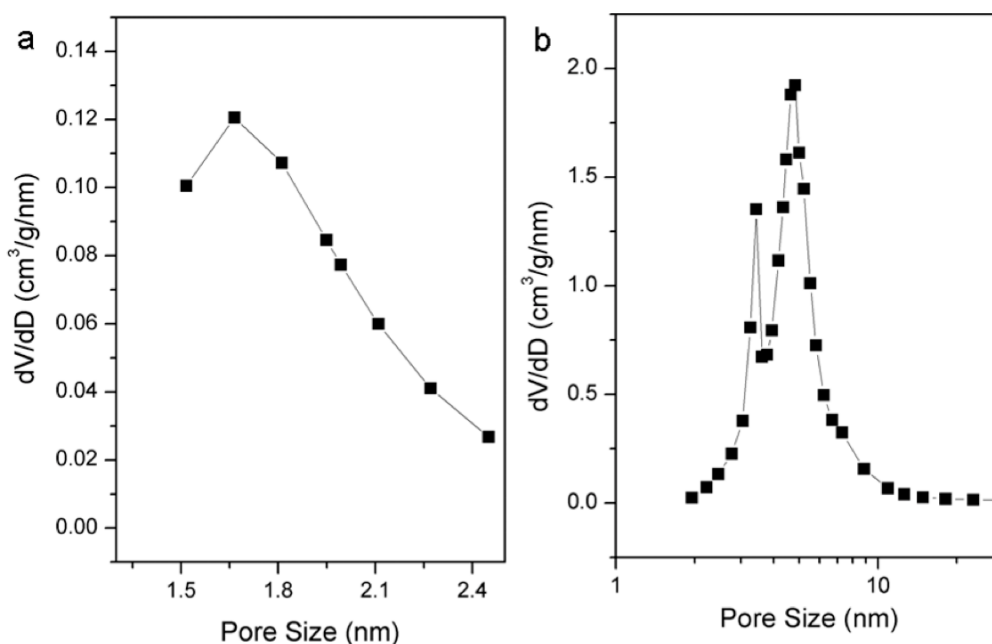


Figure S5. Pore size distribution curves of the mesoporous alumina OMA-2-FMC. (a) the small pore size distribution obtained by Dubinin-Radushkevich using the p/p_0 data smaller than 0.05 from the adsorption branch; (b) the mesopore size distribution obtained by the BJH method from the desorption branch of the N_2 sorption isotherms presented in Figure 3B. An obvious pore size distribution with a mean pore size of about 1.7 nm is observed from (a). Bi-modal mesopores are clearly observed in (b). It suggests that the mesoporous alumina OMA-2-FMC has two pore systems, originating from the primary mesochannels and the carbon walls of the template, respectively.

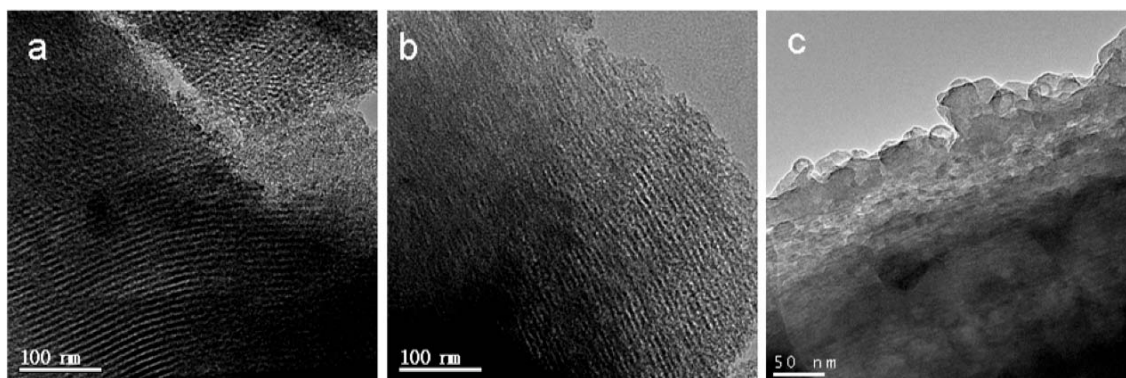


Figure S6. TEM images of the functionalized mesoporous carbon (FMC) template (a), the mesoporous alumina@carbon OMA-2@FMC composites (b), and the composites OMA-3@FMC (c), respectively. The changes of the visibility of the mesopores of the carbon parent with increasing loading of alumina can easily be observed. In image (b), the contrast difference between carbon walls and pores is not so obvious as the carbon template, while it is totally different in image c, showing an increasing filling effect.

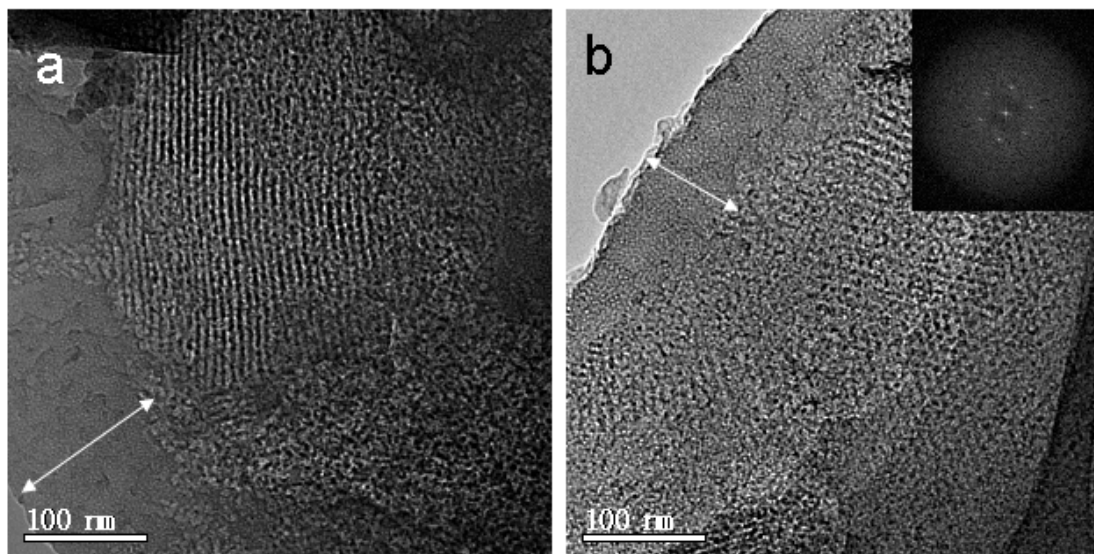


Figure S7. TEM images and inset corresponding FFT pattern of the mesoporous alumina OMA-3-FMC material. The white arrows indicate the dense surface layers of Al_2O_3 wrapping the ordered mesopore domains, showing overload of alumina precursors. The extra-alumina species are coated or dispersed on the outside surface of the mesopore walls. As a result, lower surface area and pore volume are obtained.

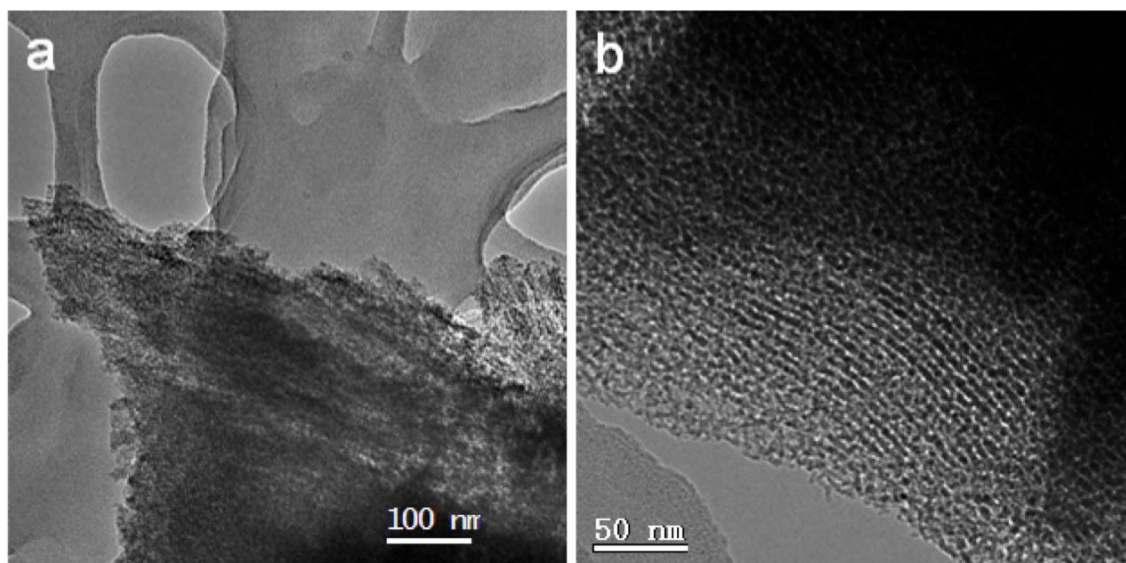


Figure S8. (a) TEM image the mesoporous alumina OMA-1-FMC material obtained with only one cycle of impregnation-conversion procedure, (b) TEM images of the ordered mesoporous alumina obtained by adopting aqueous AlCl_3 solution instead of $\text{Al}(\text{NO}_3)_3$ ethanol solution as the precursor.

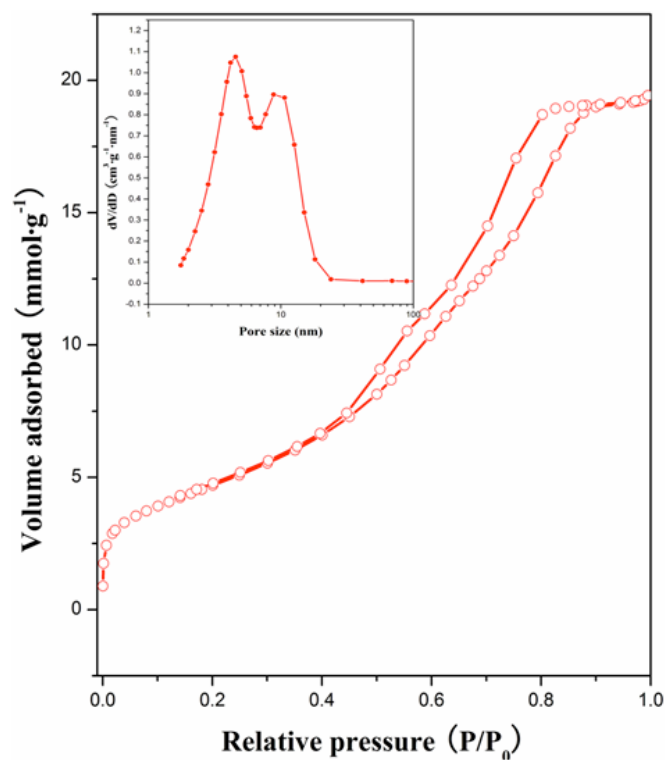


Figure S9. N₂ sorption isotherms and the corresponding pore size distribution of the mesoporous alumina material obtained with very low loading of alumina (alumina content of only about 13 wt%).

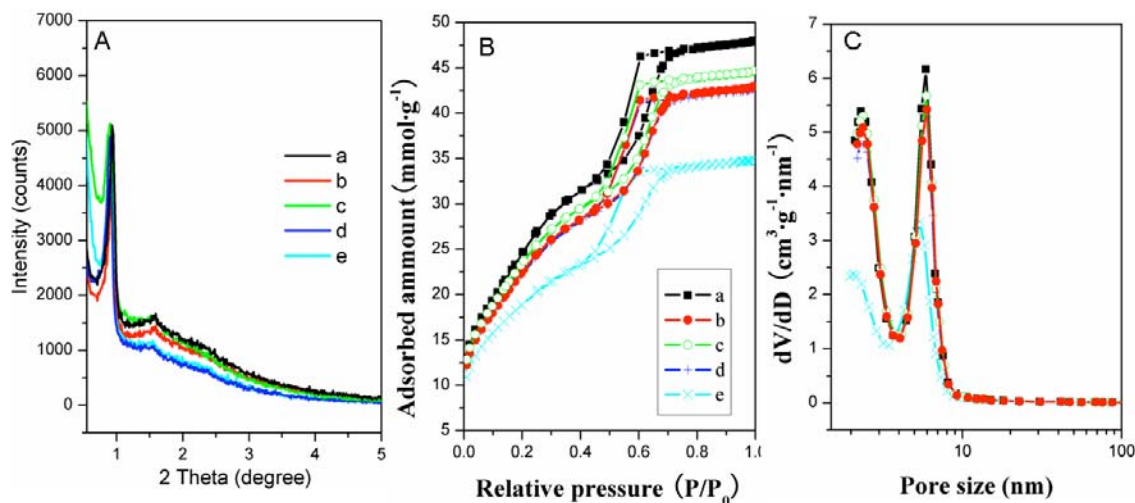


Figure S10. Small-angle XRD patterns (A), N₂ sorption isotherms (B) and the corresponding pore size distribution curves (C) of the pristine mesoporous carbon template (a) and the products after treated with a 2.5 M HNO₃ solutions at 40 °C (b) and 70 °C (d) for 3 h, and the products after being treated with a 5.0 M HNO₃ solution at 40 °C (c) and 70 °C (e) for 3 h, respectively. In order to get a functionalized mesoporous carbon template with high density of surface oxygen-containing groups as well as small structure and texture deterioration, the functionalized mesoporous carbon template was obtained by treating the pristine mesoporous carbon carbon with a 5.0 M HNO₃ solution at 40 °C for 3 h.

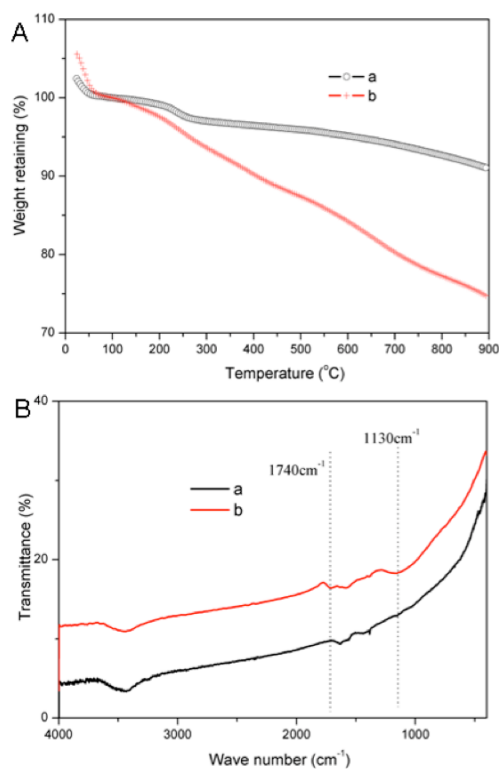


Figure S11. TG curves conducted under N₂ (A) and FTIR spectra (B) of the pristine mesoporous carbon (PMC) (a) and the functionalized carbon (FMC) template (b) functionalized with a 5 M HNO₃ solution at 40 °C for 3 h. In figure A, compared to the pristine PMC carbon, the FMC counterpart shows a significant larger amount of weight loss, indicating that a lot of surface oxygen-containing groups are generated, which changes the carbon material from mainly hydrophobic to hydrophilic. Correspondingly, in figure B, three new bands centered at 1740, 1590 and 1130 cm⁻¹ are detected, indicating the generation of surface carboxylic, hydroxyl and ether groups. Elemental analysis results revealed that the pristine carbon has 86.98 % of C, 2.22 % of H, and ~ 9.0 % of O, whereas the functionalized carbon 72.20 % of C, 1.88 % of H, and ~ 24.84 % of O, clearly suggesting the generation of surface oxides.

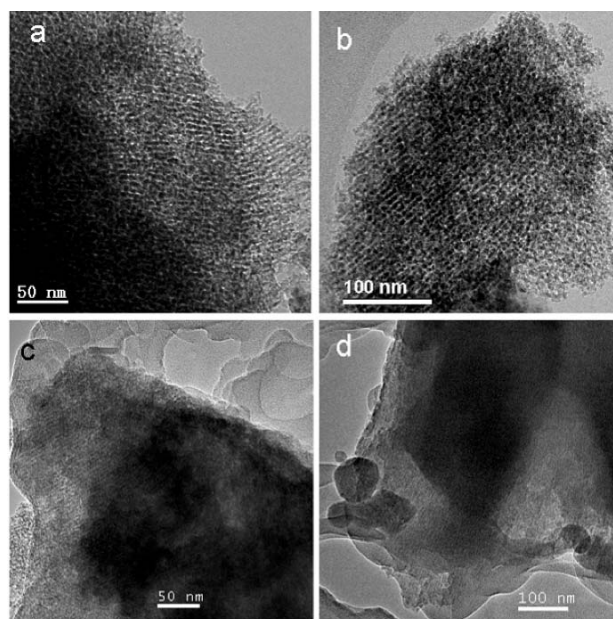


Figure S12. TEM images of the mesoporous alumina materials obtained from the direct calcination without the *in-situ* ammonia hydrolysis step. The carbon-free alumina products obtained from the alumina@carbon composites after being calcined at 600 (a), 700 (b), 800 (c) and 900 °C (d) for crystallization.

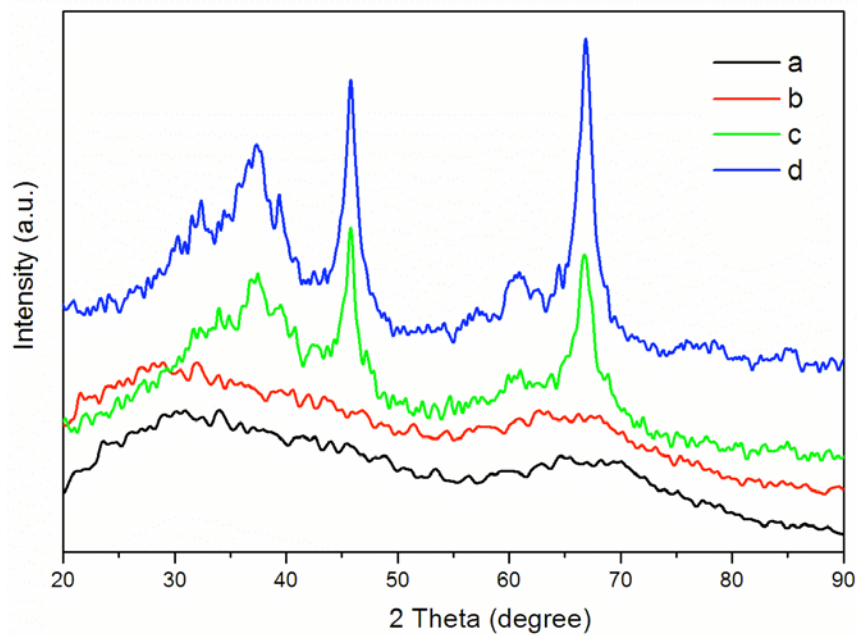


Figure S13. Wide-angle XRD patterns of the mesoporous alumina materials obtained from the direct calcination without the *in-situ* ammonia hydrolysis step. The carbon-free alumina products were obtained from the alumina@carbon composites after being calcined at (a) 600 (a), 700 (b), 800 (c) and 900 °C (d) for crystallization. The sample calcined at 900 °C shows possible partial formation of α -alumina.

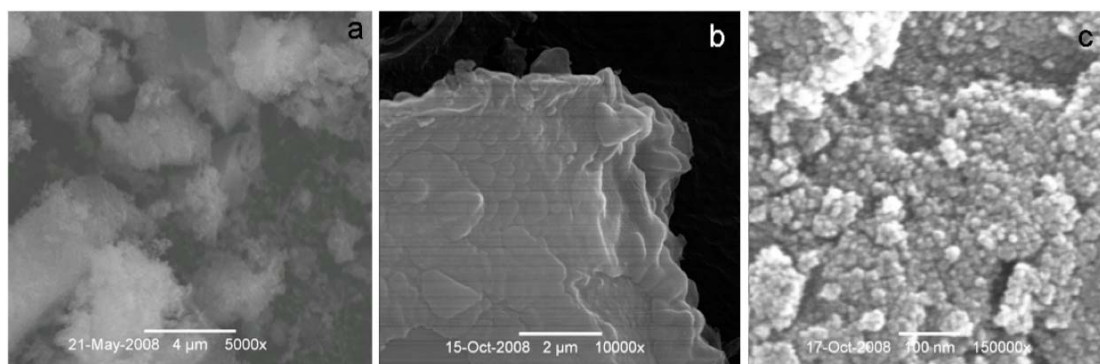


Figure S14. SEM images with different magnifications of the mesoporous alumina MA-3-PMC obtained by using the pristine mesoporous carbon as a hard-template *via* the direct calcination method without the *in-situ* ammonia hydrolysis step.

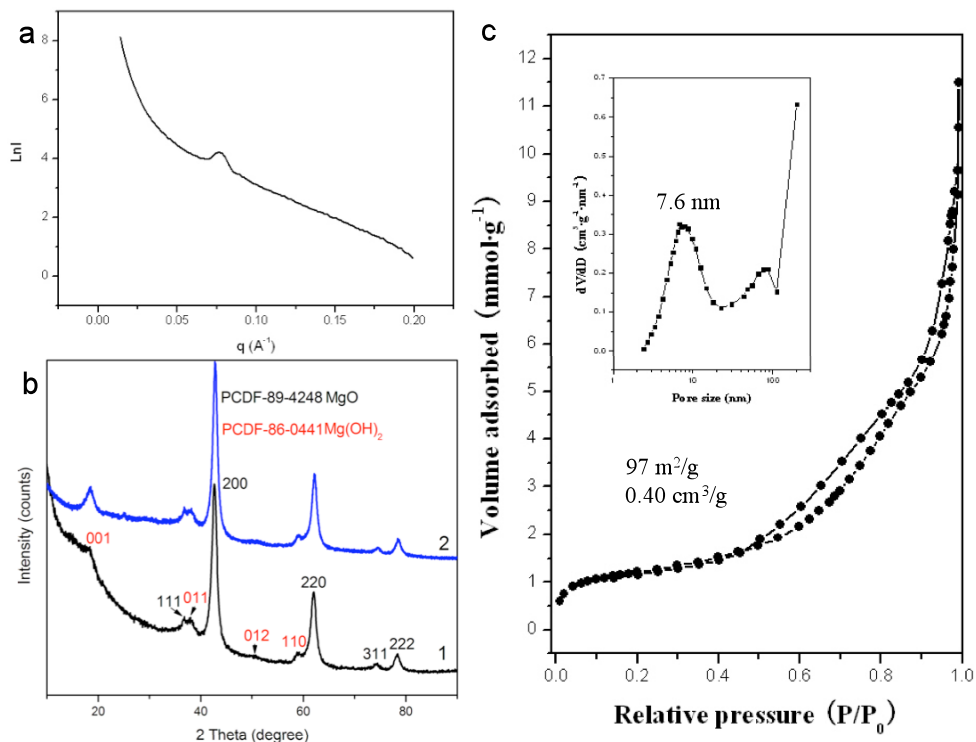


Figure S15. The SAXS (a), wide-angle XRD (b, curve 1) patterns, N_2 sorption isotherms (c) and the corresponding pore size distribution curve (inset c) of the ordered mesoporous magnesium oxide MgO-3-FMC material templated from the functionalized mesoporous carbon. From the SAXS patterns, a scattering peak is detected, showing an ordered MgO mesostructure. The wide-angle XRD pattern demonstrates the pore walls are highly crystalline with MgO as a dominant component and $\text{Mg}(\text{OH})_2$ as minor one. The N_2 sorption isotherms show a high surface area ($\sim 100 \text{ m}^2/\text{g}$) and uniform mesopores with a mean pore size of 7.6 nm. In spite of the fact that MgO is a basic agent, the mesoporous MgO is quite stable under air without reaction with carbon dioxide at ambient conditions even after a one-year time, confirmed by its similar XRD pattern (Figure S15b, curve 2) as that obtained shortly after the synthesis.

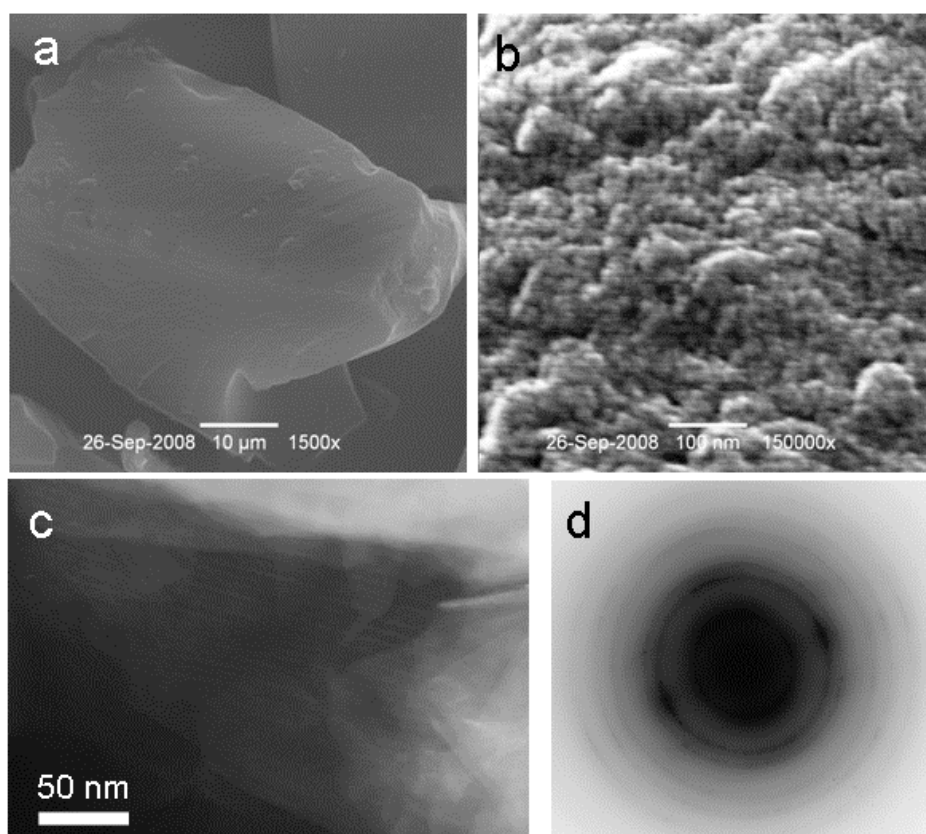


Figure S16. SEM images (a, b), TEM image (c) and SAED pattern (d) of the ordered mesoporous magnesium oxide MgO-3-FMC material. The flake-like morphology and ordered mesostructure of the carbon parent are successful inherited. The surface of the mesoporous MgO is much smoother than that of alumina.

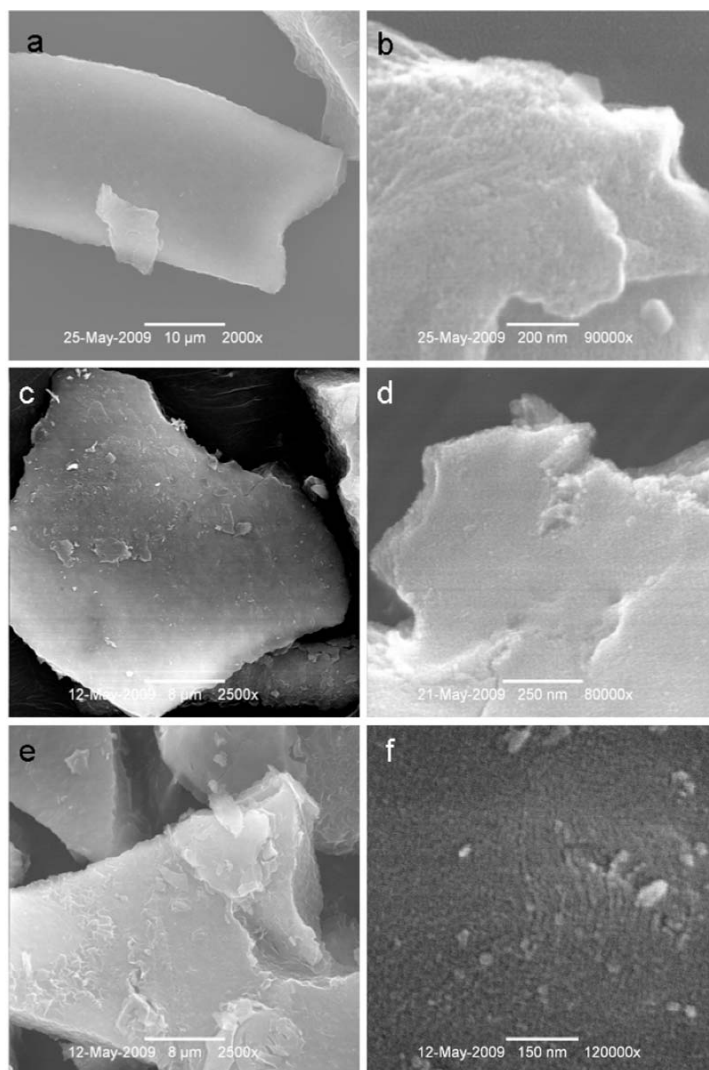


Figure S17. SEM images with low (a, c and e) and high (b, d and e) magnifications of the mesoporous alumina materials obtained by heating the mesoporous alumina OMA-3-FMC material at 700 (a, b), 800 (c, d) and 900 °C (e, f), respectively, under air for 1 h. It shows that the ordered mesostructure deteriorates a lot and the surface becomes more rough after the thermal treatment, indicating growth of crystalline grain size.

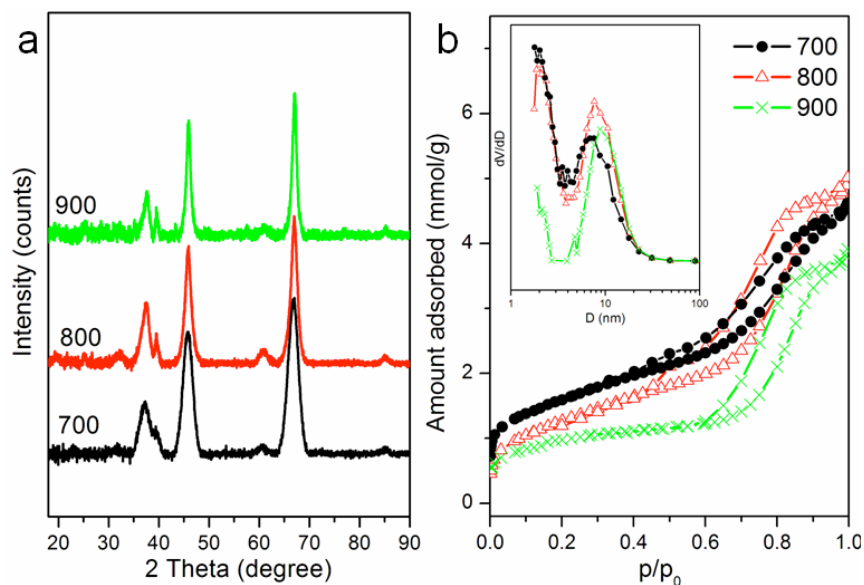


Figure S18. Wide-angle XRD patterns (a), N₂ sorption isotherms (b) and the corresponding pore size distribution curves (inset b) of the mesoporous alumina materials obtained by heating the mesoporous alumina OMA-3-FMC material at 700 ~ 900 °C under static air for 1 h. They still show nanocrystalline nature, with a growth of the particle size from 6 ~ 7 nm to 8 ~ 9 nm at 900 °C. The ordered mesostructure deteriorates a lot (data not shown) but the surface areas of the products are still high of 80 ~ 120 m²/g and the pore size distributions are narrow centered at about 2.3 and 6 ~ 8 nm, respectively.